

# Dynamics of bacteria scanning a porous environment

Ehsan Irani,<sup>1</sup> Zahra Mokhtari,<sup>2</sup> and Annette Zippelius<sup>3</sup>

<sup>1</sup>*Max Delbrück Center for Molecular Medicine in the Helmholtz Association (MDC),  
The Berlin Institute for Medical Systems Biology (BIMSB), Berlin, Germany*

<sup>2</sup>*Department of Mathematics and Computer Science, Freie Universität Berlin*

<sup>3</sup>*Institut für Theoretische Physik, Universität Göttingen*

(Dated: December 2, 2021)

It has recently been reported that bacteria, such as *E.coli* [1] and *P. putida* [2], perform distinct modes of motion when placed in porous media as compared to dilute regions or free space. This has led us to suggest an optimal strategy for active particles in a disordered environment: reorientations are suppressed in locally dilute regions and intensified in locally dense ones. Thereby the local geometry determines the optimal path of the active agent and substantially accelerates the dynamics for up to two orders of magnitude. We observe a non-monotonic behavior of the diffusion coefficient in dependence on the tumbling rate and identify a localisation transition, either by increasing the density of obstacles or by decreasing the reorientation rate.

The spreading of active particles in a complex environment has been a topic of intense research in recent years. Several experimental groups have studied the diffusion of *Escherichia coli* (*E.coli*) in porous media, such as agar [1, 3, 4]. The bacterial motion in free space is thought to be well described by run and tumble dynamics, such that straight runs are interrupted by random reorientations. Bacterial dynamics in a complex environment is less well understood and it is not clear, how and to what extent bacteria are able to adapt their activity to an inhomogeneous environment.

Local sensing of the environment has been adopted as a survival mechanism in many phyla throughout the animal kingdom. Several microorganisms regulate their behaviour according to the density of neighbours or to local gradients in phoretic propulsion. For example, a mechanism known as quorum sensing, allows bacteria to change their speed according to the density of neighbours [5–12]. Schools of fish have been observed to regulate their speed according to the density of neighbours [13, 14]. Licata et al. [4] have studied chemotaxis in porous media and suggest that the tumbling rate is changed in response to the local chemotactic concentration. Bacteria with several swimming modes, such as *P. putida* [2], can switch between different run modes in response to chemotactic conditions optimising their chemotactic strategy. Volpe and Volpe [15] argue that the topography of the environment globally enhances the random motion as compared to the ballistic one. Recent experiments by Datta et al. [1] on bacterial hopping in porous media revealed that random disorder does not just change the tumbling frequency and consequently also the run length. Instead the bacteria are able to change their dynamics, if trapped, so that hopping becomes dependent on the geometry of the pore space.

Inspired by the ability of many microorganisms to sense their local environment, we study a dynamics of active particles which depends on the local density. As an example, we consider a situation, where the active parti-

cles need to explore large regions of their environment in short times. Reorientation in dilute regions is then rather ineffective, whereas reorientation in dense regions and in particular in traps is essential. An optimal strategy requires a hopping mechanism which is guided by the local environment. We model the bacteria as rigid trimers or rods, which are known to be trapped easily, and suggest a reorientation mechanism which is sensitive to the local density of the porous medium. It is predominant only in trapped configurations and hence very efficient to accelerate the dynamics.

Several theoretical studies and simulations have addressed active particles in a random environment [16–19]. Frequently the porous medium is modeled by the Lorentz model [20, 21], where static obstacles are placed randomly in space, covering a volume (area) fraction  $\phi_o$ . Zeitz et al. [16] simulated active Brownian particles, whose diffusion constant is depressed due to the tendency of active particles to get stuck around obstacles. Reichhardt et al. [17] include a drift term; surprisingly the drift velocity is nonmonotonic as a function of run time for given  $\phi_o$ . Bertrand et al [18] compute the diffusion constant of active particles in a lattice gas model and show that the diffusion constant is nonmonotonic in the tumbling rate as long as the obstacles are static (or very slow). More recently Kurtzthaler et al. [19] derived a geometric criterion for optimal spreading, when the run length of the bacteria is comparable to the longest straight path in the porous medium. In contrast to these approaches, we suggest a **local** adaptation mechanism of the dynamics, which is most efficient in a strongly inhomogeneous environment. Adaptation to the geometrical properties of the environment is a desired feature in design of artificial active agents. Particularity if they are appointed to transportation or escaping tasks in disordered media.

*Model:* We consider the dynamics of an elongated tracer particle in a two-dimensional medium of static obstacles with area fraction  $\phi_o$ . The tracer is modeled as

a rigid trimer, consisting of 3 beads of radius  $R_t$ . The position vector of the central bead is denoted by  $\mathbf{r}$ . The two peripheral beads are rigidly attached to the central bead, forming a linear configuration, whose orientation is specified by a unit vector  $\mathbf{n} = (\cos \varphi, \sin \varphi)$ . The position vectors of the two peripheral beads are thus given by  $\mathbf{r}^\pm = \mathbf{r} \pm 2R_t\mathbf{n}$ . The trimer is considered a model for an elongated particle of aspect ratio 3. The obstacles are modelled as disks (2D), much larger than the beads of the trimer. In the following we choose for the ratio of obstacle radius to tracer radius  $R_o/R_t = 10$ . The interaction of the beads with the obstacles,  $\mathbf{F}(\mathbf{r})$ , is taken as a contact potential, modelled by a stiff spring.

Since the trimer is modelled as a rigid body, its dynamics is fully characterized by an equation for the translational motion of the center of mass, which is taken to coincide with  $\mathbf{r}$ , and an equation of motion for the orientation  $\varphi$ . We assume overdamped dynamics, according to:

$$\dot{\mathbf{r}} = \mathbf{v}_a + \frac{1}{\gamma} \sum_{i=1}^{N_o} \mathbf{F}_i. \quad (1)$$

The total force on the center of mass due to obstacle  $i$  at position vector  $\mathbf{R}_i$ , is given by  $\mathbf{F}_i = \mathbf{F}(\mathbf{r} - \mathbf{R}_i) + \mathbf{F}(\mathbf{r}^+ - \mathbf{R}_i) + \mathbf{F}(\mathbf{r}^- - \mathbf{R}_i)$ . The active velocity  $\mathbf{v}_a$  is applied along the direction of the trimer  $\mathbf{n}$ . Interactions with the obstacles cause the trimer to rotate:

$$\dot{\varphi} = \sum_{i=1}^{N_o} \tau_i. \quad (2)$$

where the torque,  $\tau_i$ , is explicitly given by  $\tau_i = (\mathbf{r}^+ - \mathbf{r}) \times \mathbf{F}(\mathbf{r}^+ - \mathbf{R}_i) + (\mathbf{r}^- - \mathbf{r}) \times \mathbf{F}(\mathbf{r}^- - \mathbf{R}_i)$ . The torque is always normal to the plane of motion and  $\tau_i$  is the projection of the vectorial torque on the normal of the plane of motion.

The occasional tumbling of bacteria has been modeled as a stochastic reorientation process. For example, the bacteria reorient in random directions with a given probability. Such a model is widely accepted for run and tumble dynamics in solution. Does it apply also in dense porous media? Recently it has been suggested [1] that bacteria are able to change their dynamics, if trapped. This has led us to introduce a reorientation mechanism which depends on the local environment of the tracer. In particular, the reorientations which disturb the ballistic motion in void space and simultaneously prevent the particles from getting trapped, are adapted to the local density in a strongly heterogeneous environment. In that way, we try to model the experimental finding that ‘‘hops are guided by the geometry of the pore space’’ [1].

Physical interactions between bacteria and surfaces are known to be determined by near-field lubrication forces [22–24] and steric collisions [25]. Bacterial responses to such interactions vary from trapping in almost deterministic circular trajectories [23] to enhanced

reorientations [26] depending on the type of surface and species.

With a rate of  $\lambda = 1/t_{re}$  the local volume fraction  $\phi_{local}$  is calculated inside a region with radius  $r_l$ , surrounding the trimer’s head (see Fig.1). We use a function  $G(\phi_{local})$  to generate the probability of performing a random reorientation in the full range from 0 to  $2\pi$ . The functional form of  $G(\phi_{local})$  incorporates the sensing mechanism which we refer to as ‘‘quorum sensing’’ in the following. Constant  $G$  results in the standard run and tumble dynamics with the rate of  $\lambda = 1/t_{re}$ , independent of the local environment. For a more sensitive function to  $\phi_{local}$  we consider a sigmoidal form as

$$G(\phi_{local}) = \frac{C}{1 + \exp^{-k(\phi_{local} - \phi_0)}} \quad (3)$$

for the reorientation probability, with  $C$  being the normalization factor. This choice reflects a high probability of reorientation in a locally dense region and a very low probability in a locally more dilute region. To approximate a step function, we choose  $k = 100$  and  $\phi_0 = 0.63$

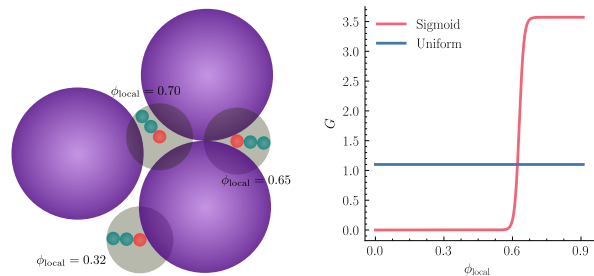


FIG. 1. Left: A hypothetical disk (shown in grey) is defined for each trimer by a concentric area of radius  $r_l$  centered around the trimer’s head. The local area fraction  $\phi_{local}$  is the overlap of the hypothetical disk with neighbouring obstacles. Right: Tumbling rate  $G/t_{re}$  for uniform (blue) and sigmoidal (red)  $G$ .

We want to analyse the dynamics of the tracer particle as a function of several parameters. Without density dependent reorientation, these are the magnitude of the active velocity  $v_a$  and the packing fraction of the obstacles  $\phi_o$ . Including density dependent reorientation, the important parameter is the time-scale  $t_{re}$  of reorientation. The size of the region,  $r_l$ , to determine the local density should be comparable to the size of the obstacle. Other functions  $G(\phi_o)$ , mapping  $\phi_{local}$  to the probability of reorientation, may be considered in future work.

The parameters can be expressed in timescales. We measure lengths in units of  $2R_t$  and times in units of the active timescale  $t_a = 2R_t/v_a$  which is controlled by the active velocity. In these units, the reorientation time

$\tau_{\text{re}} = t_{\text{re}}/t_a$  is the Peclet number. The collision time is given  $t_{\text{coll}}^{-1} = 2v_a R_o N_o/L^2$  or in dimensionless units  $t_a/t_{\text{coll}} = 2R_o R_t N_o/L^2$ . It is controlled by the area fraction  $\phi_o = N_o \pi R_o^2/L^2$ . Both tumbling as well as collisions randomize the velocity of the active particle and give rise to diffusion and hence cause a crossover from ballistic motion to diffusive motion.

We used HOOMD-Blue [27] to integrate Eq. 1 and run Molecular Dynamics simulations on GPU ( $\Delta t_{\text{MD}} = 10^{-2}$ ). Freud package [28] is used to investigate the local environment. For each set of  $(\tau_{\text{re}}, \phi_o)$ , 10 to 50 simulations are performed, each with 100 independent trimers and  $N_o = 2500$  random obstacles without overlaps.

*Results:* We focus here on the dynamics of tracer particles adapted to their local environment. In Fig. 2 we show the MSD for  $G(\phi_{\text{ocal}})$  (full line) in comparison to a constant  $G$  (dashed line). The most striking observation is the strong boost of the dynamics for quorum sensing, when the reorientation time is comparable to the timescale of active motion. The acceleration is due to uninterrupted ballistic motion as well as reduced trapping times. For moderate densities, such as  $\phi_o = 0.4$  shown in Fig. 2, the first mechanism dominates, whereas for rather dense systems such as  $\phi_o = 0.7$ , the latter dominates (see below).

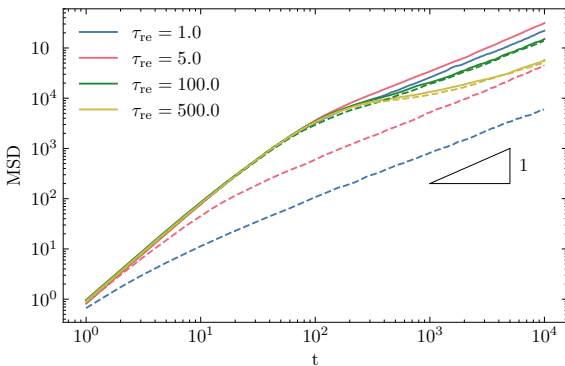


FIG. 2. MSD of trimers for  $\phi_o = 0.4$  and different reorientation times  $\tau_{\text{re}}$ ; Comparison of sigmoidal (full line) and constant  $G$  (dashed line).

It is instructive to look at the distribution of waiting times, defined as the time interval between two reorientation events. The distribution is a simple exponential for a uniform  $G$  and all densities, characterized uniquely by  $\tau_{\text{re}}$ . In contrast, sigmoidal  $G$  gives rise to a second exponential, which slows down dramatically as the density decreases, see Fig. 3a. In fact the decay rate  $\beta$  of the distribution increases approximately exponentially with  $\phi_o$ , as shown in the inset of Fig. 3a. The long relaxation times for moderate  $\phi_o$  are directly related to increasingly long straight paths for dilute systems. Following refs.[19, 29] we compute the distribution of straight paths which lie entirely in the void space of the porous medium. The

distribution of these so called chord lengths is shown in Fig. 3b. The distribution strongly resembles the distribution of waiting times and the corresponding decay rate also increases approximately exponentially with  $\phi_o$ , as shown in the inset of Fig.3b. We hence conclude that the frequency of reorientation is determined by the geometry of the environment. The latter determines the optimal path for the active particle which is further supported by the movies in the SM [30].

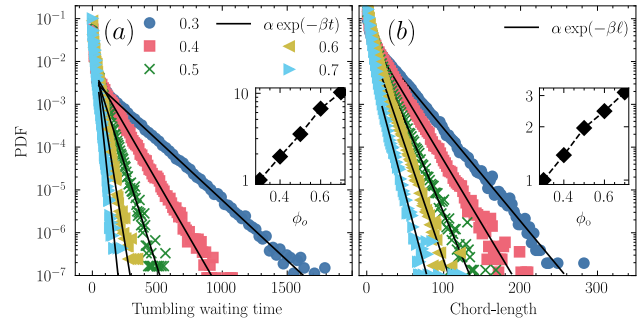


FIG. 3. (a) Distribution of waiting times between two reorientation events; inset: relaxation rate, normalized to  $\phi_o = 0.3$ . (b) Distribution of chord lengths; inset: relaxation rate, normalized to  $\phi_o = 0.3$ . All for different  $\phi_o$  and  $\tau_{\text{re}} = 5$ ;

To quantify the acceleration due to quorum sensing, we extract a diffusion constant from the long time behaviour of the MSD. It is plotted in Fig. 4 as a function of  $\tau_{\text{re}}$  for both uniform and sigmoidal  $G$ . The diffusion constant is larger by almost two orders of magnitude for quorum sensing and  $\tau_{\text{re}} \sim 1$ , i.e. when the reorientation time is comparable to the timescale of active motion. Furthermore, the diffusion constant is nonmonotonic in  $\tau_{\text{re}}$ , as already observed in Fig. 2. The fastest dynamics is found for  $\tau_{\text{re}} \sim 5$  and slows down for increasing as well as decreasing  $\tau_{\text{re}}$ . This nonmonotonic behaviour has been observed previously for constant reorientation rate [18], where it is in fact more pronounced. It can be explained by the following intuitive argument: For large  $\tau_{\text{re}}$  the particles are stuck for a long time in a locally dense region of obstacles, so that the diffusion constant is small and approximately inversely proportional to  $\tau_{\text{re}}$ . For small  $\tau_{\text{re}}$ , randomization of the active motion is fast, so that the crossover from ballistic motion to diffusive behaviour happens at early times, resulting in small values of the diffusion constant for small  $\tau_{\text{re}}$ . These two effects together give rise to an optimal value for  $\tau_{\text{re}}$ , for which the dynamics is fastest.

The difference between uniform and sigmoidal  $G$  disappears for very long reorientation times, when reorientation is so rare that ballistic motion is mainly interrupted by collision events which are the same for both models. It has been suggested recently [19] that reversing the veloc-

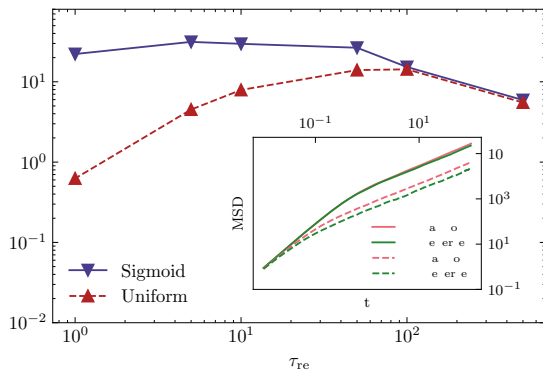


FIG. 4. Diffusion coefficient versus  $\tau_{re}$  for  $\phi_o = 0.4$ ; a sigmoidal function  $G$  (blue symbols) is compared to a constant  $G$  (red symbols); inset: MSD for a sigmoidal function  $G$  (full line) and constant  $G$  (dashed line), comparing reorientation in the form of reversals to randomly chosen angles.

ity of the active particle is an efficient means to accelerate the dynamics. In the inset of Fig. 4 we compare random reorientation and run-reverse dynamics for both constant  $G$  and quorum sensing. The enhancement of the dynamics due to quorum sensing is even stronger for run-reverse dynamics than for uniform reorientations.

Quorum sensing is expected to be most efficient in a strongly inhomogeneous environment. Here we implement a uniform distribution of obstacles and hence have chosen a moderate density  $\phi_o = 0.4$ , intermediate between a very dense system which is almost uniform and a dilute system where trapping of an active particle is rare. In the following we investigate density dependent reorientation as a function of area fraction.

The dependence of the dynamics on the area fraction of obstacles is shown explicitly in Fig. 5a. As one ex-

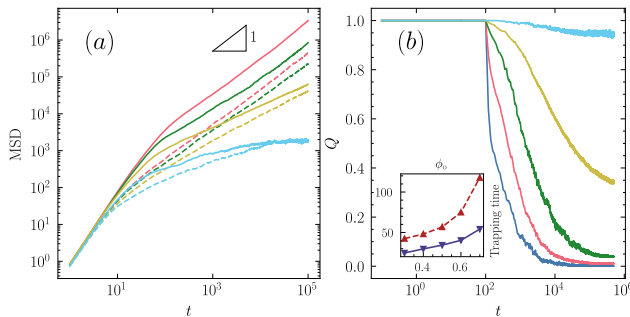


FIG. 5. (a) MSD of trimers for  $\tau_{re} = 5$  and different area fraction  $\phi_o$ ; comparison of sigmoidal (full line) and constant  $G$  (dashed line). (b)  $Q_d(t)$  for  $d = 100$ ,  $\tau_{re} = 5$  and several values of  $\phi_o$  (color coding as in Fig. 3); inset: comparison of mean trapping time for uniform (red) and sigmoidal  $G$  (blue)  $G$  as a function of  $\phi_o$ .

pects, we see ballistic motion for short times and then a

crossover to diffusion at long times. As the density of obstacles  $\phi_o$  is increased, the diffusion constant is reduced and eventually at  $\phi_o = 0.7$ , all particles are localized, exhibiting a plateau in the MSD. The size of the plateau is the average squared localisation length and independent of the dynamics. At the localisation transition, we observe subdiffusive behaviour. The critical volume fraction for localisation,  $\phi_c$ , depends on the size ratio  $R_o/R_t$ .

Even though the averaged MSD is diffusive for long times and area fractions below the critical threshold,  $\phi_c$ , this does not imply that all particles are free to diffuse through the whole system. Any finite fraction of mobile particles gives rise to an increase of the MSD, whereas the localised ones give a finite contribution to the total sum. Partial localisation is due to the existence of finite size void regions, coexisting with the macroscopic void area. In fact the size of these cages is widely distributed; for  $\phi_o = 0.6$  it varies over more than two orders of magnitude.

A quantitative measure of localised particles is provided by  $Q(t; d)$ , the fraction of particles which have moved less than  $d$  in time  $t$ . Choosing  $d = 0.3L$ , we observe that  $Q(t; d)$  decays to a finite value even well below  $\phi_o = 0.7$ , implying that a finite fraction of the particles is localised (see Fig. 5b). The fraction of localised particles,  $Q_\infty(d)$  for  $\phi_o \leq 0.7$  depends of course on the chosen value of  $d$ . In the above figure this was chosen comparable to system size in order to show that a finite fraction of particles is localised on scales comparable to system size.

The acceleration of the dynamics for quorum sensing is not only due to undisrupted ballistic motion in dilute regions, but also to a reduction of trapping times in dense regions. As we increase  $\phi_o$ , escaping from the local cages becomes increasingly more important, so that the reduction in trapping time is the dominant mechanism responsible for the speed up of transport in this regime. We follow Ref.[1] and define trapping as the time span in which the speed of the particles is less than  $v_a/2$ . The mean trapping time is reduced by a factor of approximately 2 for sigmoidal  $G$  as compared to uniform  $G$  and most pronounced for the highest densities (see inset of Fig. 5b). The reduction of trapping times as a result of local sensing is due to the efficient untrapping mechanism: whereas for uniform  $G$  particles reorient as much close to the inner boundaries and dead ends of the cage as they do in the center of the cage, for sigmoidal  $G$  they effectively reorient only at dead ends, resulting in a negligible number of reorientations, unless it is necessary to escape a trap.

Localisation can also occur for smaller  $\phi_o$ , such as  $\phi_o = 0.4$ , if the reorientation time is increased accordingly. This is apparent in Fig. 2, where we observe the emergence of a plateau for  $\phi_o = 0.4$  and  $\tau_{re} \geq 500$ . It is more clearly seen in a plot of the distribution of displacements for two different values of  $\tau_{re}$ , shown in the SM.

Increasing  $\tau_{re}$  thus provides another route to the glassy dynamics in active matter (See Fig. 1 in SM [30]).

We have introduced a model for bacterial spread in a porous medium, which substantially accelerates the dynamics. It is based on a sensing mechanism of the local density and thereby reduces adverse tumbling in locally dilute regions and enhances necessary reorientations, when the bacteria are trapped in local cages. The extremely long waiting times between successive tumbling events for moderate densities can be traced to the geometry of the porous structure which determines the optimal path of the active agent. For the fully random structure under consideration, the diffusion constant can be enhanced by two orders of magnitude. We expect the effect to be even stronger in a structured system whose inhomogeneities extend over finite length-scales.

The model can be easily extended to other transport phenomena which require scanning of the environment. A prominent example is chemotaxis, requiring local sensing of food or poison. Here a concentration dependent tumbling rate may by the simplest model to account for directed motion in a concentration gradient.

E.I acknowledges support from the Helmholtz Association (Germany), core funding to the Pombo group and computational resources at MDC. Z.M would like to acknowledge Germany's Excellence Strategy – MATH+ : The Berlin Mathematics Research Center (EXC-2046/1) for partial support of this project.

- 
- [1] T. Bhattacharjee and S. Datta, *Nature Communications* **10**, 1 (2019).
- [2] Z. Alirezaeizanjani, R. Großmann, V. Pfeifer, M. Hintsche, and C. Beta, *Science advances* **6**, eaaz6153 (2020).
- [3] A. Wolfe and H. Berg, *Proc. Nat. Acad. Sci. USA* **86**, 6973 (1989).
- [4] N. Licata, B. Mohari, C. Fuqua, and S. Setaysehgar, *Biophys. J.* **110**, 247 (2016).
- [5] C. Liu and et al., *Science* **334**, 238 (2011).
- [6] X. Fu, L.-H. Tang, C. Liu, J.-D. Huang, T. Hwa, and P. Lenz, *Phys. Rev. Lett.* **108**, 198102 (2012).
- [7] M. Cates, D. Marenduzzo, I. Pagonabarraga, and J. Tailleur, *Proc. Nat. Acad. Sci. USA* **107**, 11715 (2010).
- [8] T. Bäuerle, A. Fischer, T. Speck, and C. Bechinger, *Nature communications* **9**, 1 (2018).
- [9] C. A. Velasco, M. Abkenar, G. Gompper, and T. Auth, *Physical Review E* **98**, 022605 (2018).
- [10] A. Fischer, F. Schmid, and T. Speck, *Physical Review E* **101**, 012601 (2020).
- [11] M. Rein, N. Heinß, F. Schmid, and T. Speck, *Physical review letters* **116**, 058102 (2016).
- [12] M. B. Miller and B. L. Bassler, *Annual Reviews in Microbiology* **55**, 165 (2001).
- [13] Y. Katz, K. Tunstrom, C. Ioannou, C. Huepe, and I. Couzin, *Proc. Nat. Acad. Sci. USA* **46**, 18720 (2011).
- [14] S. Mishra, K. Tunstrom, I. Couzin, and C. Huepe, *Phys. Rev. E* **86**, 011901 (2012).
- [15] G. Volpe and G. Volpe, *Proc. Nat. Acad. Sci. USA* **114**, 11350 (2017).
- [16] M. Zeitz, K. Wolff, and H. Stark, *The European Physical Journal E* **40**, 23 (2017).
- [17] C. Reichhardt and C. O. Reichhardt, *Physical Review E* **90**, 012701 (2014).
- [18] T. Bertrand, Y. Zhao, O. Benichou, J. Tailleur, and R. Voiturez, *Phys. Rev. Lett.* **120**, 198103 (2018).
- [19] C. Kurzthaler, S. Mandal, T. Bhattacharjee, S. S. Datta, H. A. Stone, *et al.*, arXiv preprint arXiv:2106.05366 (2021).
- [20] F. Höfling, T. Munk, E. Frey, and T. Franosch, *The Journal of chemical physics* **128**, 164517 (2008).
- [21] T. Bauer, F. Höfling, T. Munk, E. Frey, and T. Franosch, *The European Physical Journal Special Topics* **189**, 103 (2010).
- [22] A. P. Berke, L. Turner, H. C. Berg, and E. Lauga, *Physical Review Letters* **101**, 038102 (2008).
- [23] D. Takagi, J. Palacci, A. B. Braunschweig, M. J. Shelley, and J. Zhang, *Soft Matter* **10**, 1784 (2014).
- [24] O. Sipos, K. Nagy, R. Di Leonardo, and P. Galajda, *Physical review letters* **114**, 258104 (2015).
- [25] K. Drescher, J. Dunkel, L. H. Cisneros, S. Ganguly, and R. E. Goldstein, *Proceedings of the National Academy of Sciences* **108**, 10940 (2011).
- [26] M. Molaei and J. Sheng, *Scientific reports* **6**, 1 (2016).
- [27] J. A. Anderson, J. Glaser, and S. C. Glotzer, *Computational Materials Science* **173**, 109363 (2020).
- [28] V. Ramasubramani, B. D. Dice, E. S. Harper, M. P. Spellings, J. A. Anderson, and S. C. Glotzer, *Computer Physics Communications* **254**, 107275 (2020).
- [29] S. Torquato and B. Lu, *Phys. Rev. E* **47**, 2950 (1993).
- [30] Supplementary Materials: Movies and extra plots regarding the trimer's displacements and glassy dynamics.

# Dynamics of bacteria scanning a porous environment: Supplementary Materials

Ehsan Irani,<sup>1</sup> Zahra Mokhtari,<sup>2</sup> and Annette Zippelius<sup>3</sup>

<sup>1</sup>Max Delbrück Center for Molecular Medicine in the Helmholtz Association(MDC),  
The Berlin Institute for Medical Systems Biology (BIMSB), Berlin, Germany

<sup>2</sup>Department of Mathematics and Computer Science, Freie Universität Berlin

<sup>3</sup>Institut für Theoretische Physik, Universität Göttingen

(Dated:)

## MOVIES

The movies illustrate the qualitative difference between the transport of trimers with density-dependent and uniform reorientations in porous media. To study the single agent behavior in porous media we have turned off the interaction between different trimers. In following movies  $\phi_o$  and  $G$  vary while  $\tau_{re} = 5.0$ :

- Sigmoidal G: Here  $G$  is a sigmoidal function of the local density, as given by Eq. 3 in the main text. Active trimers traverse large distances almost ballistically and reorient almost only at dead ends, where two obstacles form a wedge-shaped trap.

– [phi\\_obs0.4-sigmoid.webm](#)

– [phi\\_obs0.6-sigmoid.webm](#)

- Constant G: Here  $G$  is a constant, giving rise to uniform reorientations. The trimers do not sense the environment and reorient with equal probability in the void space or in local cages.

– [phi\\_obs0.4-uniform.webm](#)

– [phi\\_obs0.6-uniform.webm](#)

For trimers with sigmoidal  $G$ , the scanning area around the trimer is displayed by a disk colored by the value of  $\phi_{local}$ : Blue for small values, white for intermediate values and red for high values. OVITO [1] is used to visualize simulations and make movies.

## GLASSY DYNAMICS

The fraction of localised particles is quantified by  $Q(t; d)$ . It is displayed in Fig. 1 for  $d = 0.3L$  at  $\phi_o = 0.4$ . We observe an intermediate plateau and a second relaxation resembling the glassy dynamics for large reorientation times,  $\tau_{re} \geq 500$ . The decay time  $\tau_Q$  is defined as the time at which  $Q(\tau_Q) = 0.6$ . Fig. 2 exhibits the non-monotonic dependence of  $\tau_Q$  on reorientation time  $\tau_{re}$  for both constant and sigmoidal  $G$ .

Fig. 3 exhibits the distributions of particle displacements at  $t = 10^4$ . Large reorientation time results in localisation of most of the trimers. However, finite fraction

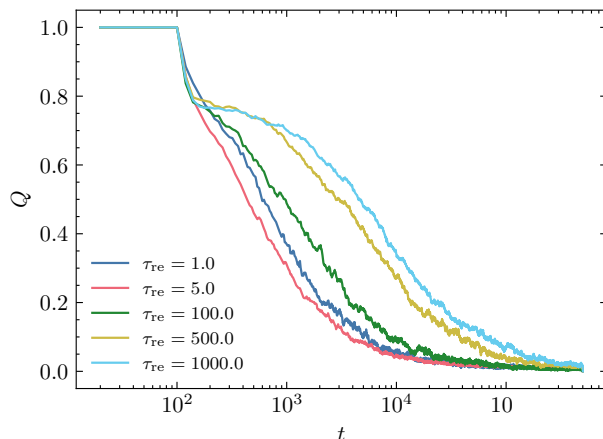


FIG. 1.  $Q_d(t)$  for  $d = 100$ ,  $\phi_o = 0.4$  and several values of  $\tau_{re}$ .

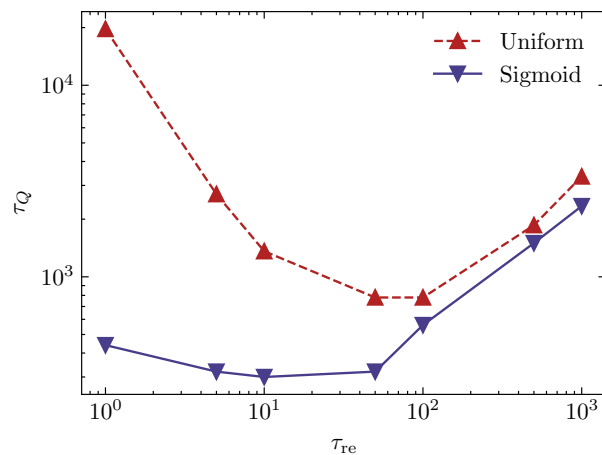


FIG. 2.  $\tau_Q$  versus  $\tau_{re}$  for systems with uniform or sigmoidal  $G$  at  $\phi_o = 0.4$ .

of trimers remain localised with decreasing the reorientation time, even at  $\tau_{re} = 5.0$  where the highest diffusion coefficient is observed.

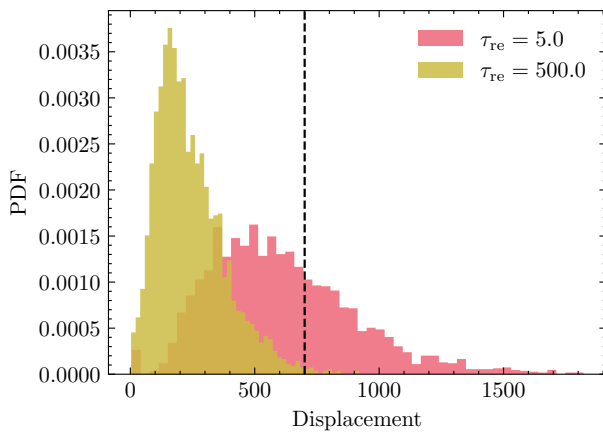


FIG. 3. Distribution of the displacements at  $t = 10^4$  at  $\phi_o = 0.4$  for two values of  $\tau_{re}$ , revealing the localisation of the trimers at large  $\tau_{re}$ . The dashed line indicates the size of the periodic box.

- 
- [1] A. Stukowski, Visualization and analysis of atomistic simulation data with OVITO-the Open Visualization Tool, *MODELLING AND SIMULATION IN MATERIALS SCIENCE AND ENGINEERING* **18**, [10.1088/0965-0393/18/1/015012](https://doi.org/10.1088/0965-0393/18/1/015012) (2010).